



Published in final edited form as:

J Med Chem. 2009 August 27; 52(16): 5164–5175. doi:10.1021/jm900473p.

Improving Metabolic Stability By Glycosylation: Bifunctional Peptide Derivatives That Are Opioid Receptor Agonists and Neurokinin 1 Receptor Antagonists

Takashi Yamamoto[†], Padma Nair[†], Neil E. Jacobsen[†], Josef Vagner[†], Vinod Kulkarni[†], Peg Davis[‡], Shou-wu Ma[‡], Edita Navratilova[‡], Henry I. Yamamura[‡], Todd W. Vanderah[‡], Frank Porreca[‡], Josephine Lai[‡], and Victor J. Hruby^{†,*}

[†]Department of Chemistry, and Pharmacology, University of Arizona, Tucson, AZ, 85721, USA

[‡]Department of Pharmacology, University of Arizona, 1501 N. Campbell Ave. Tucson, AZ 85724

Abstract

In order to obtain a metabolically more stable analgesic peptide derivative, *O*- β -glycosylated serine (Ser(Glc)) was introduced into TY027 (Tyr-*D*-Ala-Gly-Phe-Met-Pro-Leu-Trp-NH-3',5'-Bzl(CF₃)₂) which was a previously reported bifunctional compound with delta/mu opioid agonist and neurokinin-1 receptor antagonist activities, and with a half life of 4.8 h in rat plasma. Incorporation of Ser(Glc) into various positions of TY027 gave analogues with variable bioactivities. Analogue **6** (Tyr-*D*-Ala-Gly-Phe-Nle-Pro-Leu-Ser(Glc)-Trp-NH-3',5'-Bzl(CF₃)₂) was found to have effective bifunctional activities with a well-defined conformation with two β -turns based on the NMR conformational analysis in the presence of DPC micelles. In addition, **6** showed significant improvement in its metabolic stability (70 \pm 9 % of **6** was intact after 24 h incubation in rat plasma). This improved metabolic stability, along with its effective and delta selective bifunctional activities, suggests that **6** could be an interesting research tool and possibly a promising candidate as a novel analgesic drug.

Keywords

bifunctional peptide derivatives; glycopeptides; analgesics; opioid induced tolerance; opioid receptor agonist; neurokinin-1 receptor antagonist; conformation-activity relationships; NMR structure; DPC micelles

Introduction

Endogenous peptides play important roles in the maintenance of homeostasis as hormones and neurotransmitters in both the periphery and the central nerve system (CNS). Indeed, the biochemical degradation of endogenous peptides appears to be an aspect in their roles as signal-transmitters since, in many cases, protease degradation changes them into an inactive form after the signal has been appropriately transferred. However, the rapid degradation of peptides is undesirable for analgesic drugs, since generally it is desirable that the effects should last for a longer period in order to maintain effective therapeutic potency. Thus, despite their effective potentials, as well as their low toxicities, endogenous peptides have been rarely used in clinical treatment of pain, primarily due to their poor metabolic

*To whom correspondence should be addressed. Tel: (520)-621-6332, Fax: (520)-621-8407, hruby@email.arizona.edu.

Supporting Information Available: HR-MS, TLC, HPLC and ¹H-NMR data of the peptides **2-6**. The metabolic stability of peptides **3** and **4** in rat plasma. This material is available free of charge via the Internet at <http://pubs.acs.org>.

stabilities, which limits the delivery of periphery administered peptides into the site of action. Moreover, the blood-brain barrier (BBB), which is a protective barrier of the CNS, possesses membrane-bound oxidative enzymes and peptidases which degraded peripherally administered peptide drugs before they reach the CNS.¹ Therefore, a peptide drug possessing good metabolic stability together with an effective therapeutic potential should be a promising candidate for novel types of drugs.

To date, several studies have shown that the glycosylation of a peptide can provide a significant increase in stability and other biological properties,²⁻⁵ although in some cases the introduction of hydrophilicity into these molecules can result in a decrease or even loss of bioactivities.^{6,7} Other reports have shown that the glycosylation of short peptides can change tissue distribution patterns⁸⁻¹⁰ and enhance peptide-membrane interactions¹¹ compared to the original non-glycosylated sequences. In fact, we have shown that the introduction of a glycosylated residue into enkephalin derivatives leads to the enhanced biodistribution of a peptide into the brain which show better analgesic efficacies compared to the non-glycosylated enkephalins.^{5, 12-15} Glycosylation can also modify the molecular structure of a synthetic peptide in both the aqueous phase and membrane-like environments,^{16, 17} to a change in the molecular structure which has significant effects on the pharmacological and metabolic properties of bioactive peptides.¹⁸

In the present study, we report the design, synthesis and biological evaluation for a series of glycosylated peptide derivatives, to examine the effect of glycosylation on metabolic stability, bioactivity and pseudo-membrane-bound conformation for targeting analgesic peptides in comparison with the non-glycosylated derivatives. The peptide design was based on our developing bifunctional concept, in which the molecule has both an opioid agonist pharmacophore at the *N*-terminal portion and a NK1 antagonist pharmacophore at the *C*-terminus (Figure 1).¹⁹⁻²¹ This concept was based on the important observations that the simultaneous administration of opioid agonist and NK1 antagonist provided significant benefit of enhanced antinociceptive potency in acute pain states and in preventing opioid-induced tolerance in chronic preclinical trials.²²⁻²⁶ Therefore, the developing bifunctional compounds should be expected to show enhanced analgesic effects without showing the undesirable adverse effects and thus be a drug candidate for pain control.¹⁹⁻²¹ For the best bioactivity profile for the δ/μ opioid receptor ligands, a compound that is a δ opioid receptor preferring agonist may possess potential clinical benefits compared to the ones for a μ opioid receptor agonist in terms of the greater relief of neuropathic pain,²⁷ reduced respiratory depression,²⁸ and constipation²⁹ as well as a minimal potential for the development of physical dependence.³⁰ Thus, a new generation of opioid agonist with selectivity and efficacy for δ -opioid receptors over μ -opioid receptors, should display reduced toxicity and abuse potential coincident with therapeutic use. In fact, our lead bifunctional compounds, TY005 (Tyr¹-D-Ala²-Gly³-Phe⁴-Met⁵-Pro⁶-Leu⁷-Trp⁸-O-3',5'-Bzl(CF₃)₂)³¹ and TY027 (**1**: Tyr¹-D-Ala²-Gly³-Phe⁴-Met⁵-Pro⁶-Leu⁷-Trp⁸-NH-3',5'-Bzl(CF₃)₂)^{20, 32} have been shown to reverse neuropathic pain without producing opioid-induced tolerance, which validates our hypothesis that opioid agonist/NK1 antagonist bifunctional ligands would be as effective in treating neuropathic pain.

In our present drug design, Nle, which is a bioisoster of Met with high resistance to oxidation,³³⁻³⁵ was first introduced into the fifth position of **1** to provide **2**, which could be considered as a biological and physicochemical isoster of **1** with improved metabolic stability (Figure 1). Further glycosylation was made on **2** with *O*- β -glucosylated serine (Ser(Glc)) which was incorporated or inserted into residues 5, 6, 7 or 8 of **2** to form four novel carbohydrate derivatives **3-6** (Figure 1). The biological activities of the synthesized bifunctional glycopeptides (**3-6**) were extensively evaluated on our well-established radioligand binding assays, GTP γ S binding assays, and isolated tissue-based functional

assays using guinea pig ileum (GPI) and mouse isolated vas deferens (MVD) tissues.¹⁹⁻²¹ The metabolic stability of the synthesized derivatives were tested by incubation in rat plasma at 37 °C. Since understanding membrane-bound structures of ligands and ligand-membrane interactions is indispensable for further insight into their diverse biological behaviors,²⁰ the NMR structures of synthesized glycopeptides **3-6** were obtained using distance and ϕ dihedral angle constraint information in membrane-mimicking DPC micelles,^{20, 36, 37} to evaluate the biological and conformational effect of site-specific glycosylation. Further NMR studies using the paramagnetic agent Mn^{2+} were conducted to clarify the specific interactions of the glycopeptides with model cell membranes.^{15, 20, 38}

Results and Discussion

Peptide Synthesis

The glycopeptide derivatives **3-6** were synthesized using the reductive amination technique on a 4-(4-Formyl-3-methoxyphenoxy)butyryl AM (FMPB-AM) resin, which is a common solid support for carboxamides,³⁹ using the N^{α} -Fmoc solid-phase peptide synthesis (SPPS) strategy. First, an excess amount of 3',5'-bis-trifluoromethylbenzyl amine was introduced on the resin in the presence of $NaBH(OAc)_3$ and trimethylorthoformate (TMOF) for converting the aldehyde moiety of FMPB-AM resin to the corresponding secondary amine. The obtained resin-bound 3',5'-bistrifluoromethylbenzyl amine was reacted with N^{α} -Fmoc-Trp(N^{in} -Boc)-OH using HCTU in the presence of 2,6-lutidine, followed by treatment with 20% piperidine to remove the N^{α} -Fmoc protecting group. Couplings of the following protected amino acids were carried out with standard *in situ* activating reagents HCTU, in the presence of DIEA, to generate Cl-HOBt esters. Fmoc-Ser(O- β -D-Glc(OAc)₄)-OH,⁴⁰ Fmoc-Leu-OH, Fmoc-Pro-OH, Fmoc-Nle-OH, Fmoc-Phe-OH, Fmoc-Gly-OH and Boc-Tyr(tBu)-OH were used for respective coupling as protected amino acids. The removal of the acetyl protecting groups on glucose was accomplished with 80% $H_2NNH_2 \cdot H_2O$ in methanol,¹⁵ and then the resin was treated with TFA/TIPS-OTf/thioanisole (9 : 2 : 1; v/v) to obtain the corresponding crude glycopeptide derivative which was treated with 2 N NH_4F solution followed by triethylamine. The obtained glycopeptide derivative was purified on a C-18 reversed phase silica gel column followed by RP-HPLC purification, (> 98 %). The final purified peptides were characterized by analytical HPLC, ¹H-NMR, HRMS and TLC. ¹H-NMR studies showed *cis/trans* isomerization at the Pro⁶ residue in some peptides. The ratios of the *cis/trans* isomers and their assignments are available in the Supporting Information. Compound **2** was synthesized as previously described.²⁰

Biological activities

The initial biological evaluations were performed on the bifunctional peptide **2**, in which Met⁵ of **1** was substituted by Nle, to confirm their bioisosterism. As expected, almost all the bioactivities of **2** were within or close to the experimental error range of **1** (Tables 1-3). Although the only major difference was found in the E_{max} values at δ -opioid receptors in the GTP γ S binding assays (60 and 121 % for **1** and **2**, respectively), these two compounds had very similar bioactivities. Thus, the biologically active conformation of **2** was expected to be comparable to that of **1**. As also expected, **2** degraded more slowly in rat plasma than **1** did (Figure 2). Because of this improvement in terms of metabolic stability, carbohydrate residues were incorporated into the sequence of **2**.

The substitution of the fifth position in the sequence of **2** by Ser(Glc) (**3**) resulted in a large decrease in binding affinities at both δ and μ opioid receptors with only 4.4-fold δ -selectivity ($K_i = 59$ and 260 nM, respectively; Table 1). This trend in the opioid selectivity was maintained in the GTP γ S binding assays, and also in the isolated tissue bioassays using the MVD and GPI, suggesting the importance of the fifth position for both μ and δ opioid

agonist activities (Tables 2 and 3).¹⁹ Next, the Ser(Glc) was substituted for Pro at the sixth position (**4**), which was reported to be an important residue for affinity at the NK1 receptors,⁴¹ but also influenced the opioid receptors as well. The affinity of **4** at the δ opioid receptor was reduced ($K_i = 36$ nM) with very low affinity for the μ opioid receptor ($K_i = 3400$ nM). GTP γ S binding assays also gave decreased activities at both the δ and μ opioid receptors ($EC_{50} = 51$ and 380 nM, respectively) with efficient E_{max} values (134 and 81 % for δ and μ opioid receptors, respectively). Interestingly, and different from the binding assay results for the receptors, the IC_{50} value of **4** in the MVD tissue assay showed almost the same potency as **1** and **2**, with better activity in the GPI assay (18 and 250 nM for MVD and GPI assays, respectively). This might be due to the difference of efficacy requirement in the isolated tissue.

The replacement with Ser(Glc) at the seventh position (compound **5**) yielded a good result for radioligand binding assays at both the δ and μ opioid receptors ($K_i = 3.7$ and 8.0 nM, respectively, Table 1) relative to those of **3** and **4**. The binding affinity of **5** at the μ opioid receptor was 3.8-fold higher than that of **2**, whereas its affinity at the δ receptor was 3.7 times lower, leading to a ligand with only modest δ -selectivity (2.2-fold). This selectivity was maintained in the GTP γ S binding assays, but its IC_{50} in the MVD tissue was 13 nM with 40-fold selectivity over the one in the GPI assay (Tables 2 and 3). As a result, the glycopeptide with Ser(Glc)⁷ (**5**) had the same levels of functional activities to those of **2** in the isolated tissues, and gave the best affinities and activities among the three glycosylated octapeptides **3-5**. It should be noted that the direct modifications of **4** and **5** were made within the NK1 antagonist pharmacophores which is located in the C-terminal half of these peptides, and thus **2**, **4** and **5** had the same sequence for the opioid pharmacophore. However, the binding affinities of **4** and **5** at the opioid receptors, especially the affinity of **4** at the μ opioid receptors, showed the changes from those of **2**. This change may be due to the glycosylation-induced conformational change in the N-terminal halves where the opioid pharmacophore was incorporated, or a direct steric effect of the introduced sugar moiety could make some contribution in the binding. Finally, the insertion of Ser(Glc) between Leu⁷ and Trp⁸ in the sequence of **2** produced **6** which showed increased opioid affinities at δ receptors, resulting in the best affinity and δ -selectivity among the synthesized glycopeptides **3-6** ($K_i = 0.77$ and 30 nM for δ and μ opioid receptors, respectively). The K_i values of **6** for δ and μ opioid receptors were within or close to the error range of the corresponding values of **2**, suggesting that the insertion of Ser(Glc)⁸ influenced the three-dimensional conformation of the opioid pharmacophore less than for **3-5**. The compound **6** showed 49 % agonist efficacy at the δ opioid receptor compared to the standard compound (DPDPE) and the observed highly δ -selective binding affinity was consistent with the results in the isolated tissue-based assays ($IC_{50} = 17$ and 670 nM in the MVD and GPI assays, respectively). Thus **6** could be regarded as an effective opioid agonist with the highest δ -selectivity among **1-6**.

The binding affinities (K_i values) at the hNK1 receptors of **5** and **6**, whose residues next to Trp were glycosylated, were good (77 and 52 pM, respectively, Table 1), but decreased from those of **1** and **2**. The affinities of **5** and **6** at the rNK1 receptor also were less than those of **1** and **2**. These biological shifts were reasonable, since the sterically hindered glucose moiety could interact spatially with the neighboring Trp, which is a critical pharmacophore for binding to the NK1 receptors.⁴¹ However, the activities of **5** and **6** against substance P stimulation in the GPI tissue were higher than those of **1** and **2** ($K_e = 1.8$ and 8.4 nM for **5** and **6**, respectively), while **3**, which had the Ser(Glc) at the fifth position far from Trp⁸, showed 10-fold higher affinity for the hNK1 receptor ($K_i = 1.1$ pM) than **2**. The affinity of **3** at the rNK1 receptor was 5600-fold lower than the K_i value at the hNK1 receptor ($K_i = 1.5$ nM) and its activity in the GPI was consistent with the binding affinity at the rNK1

receptors. The general explanation of such a difference in the NK1 antagonist activities between different species has been provided previously by the known homology differences between rat, human and guinea pig NK1 receptors: it is well known that the human NK1 receptor has higher homology to the guinea pig NK1 receptor than to the rat or mouse NK1, and some NK1 antagonists have large species differences consistent with the reported homology.^{42, 43} However, our results suggested that the known species difference does not give a sufficient explanation in the case of these bifunctional peptides, independent of the presence or absence of a glycosylated residue. These significant differences may suggest that these peptides have affinities for guinea pig NK1 receptor similar to those for the rNK1 receptor.

The Pro⁶ was reported to play an important role for hNK1 affinity,^{41, 44} and thus the replacement of Pro⁶ with Ser(Glc) resulted in a ligand with 640 times less affinity at the hNK1 receptor compared to that of **2** (**4**; $K_i = 1.8$ nM). According to a reported modeling study,⁴² the Trp-derived NK1 antagonist L-732,138 (Ac-Trp-O-3',5'-Bzl(CF₃)₂) binds at the transmembrane domain of hNK1 receptor with a great deal of tolerance for substitution of its acetyl group which was directed toward the extracellular region. Although a large binding tolerance was expected, the Ser(Glc)⁶ incorporation in **4** might induce changes in the three-dimensional structure. **4** also had the lowest K_e value in the GPI tissue among the glycopeptides **3-6** (18 nM; Table 3). As for the species difference between the hNK1 and rNK1 receptors, all the synthesized glycopeptide derivatives **3-6** showed higher affinities at the hNK1 than at the rNK1 receptor (Table 1). It should be noted that **4** showed only a 13-fold difference between species, whereas the other glycopeptide derivatives (**3**, **5** and **6**) showed at least 180 times better affinities for the hNK1 receptors than for the rNK1, suggesting the importance of Pro⁶ for the ligand at the hNK1 receptors. **4** also had the smallest species difference between human and guinea pig NK1 receptors, implying that the incorporation of Ser(Glc)⁶ or the removal of Pro⁶ has an important effect on the species differences in binding at the NK1 receptors.

Considering both the opioid agonist and NK1 antagonist activities, the glycosylation at the position next to the Trp showed the best results (**5** and **6**) with good opioid affinities and activities together with effective potency at the NK1 receptors. Thus, the metabolic stabilities of **5** and **6** were evaluated to estimate the effect of glycosylation and to compare with those of the peptides possessing no glycosylated residue (**1** and **2**), by incubation in rat plasma at 37°C (Figure 2). The degradation curve of **5** was improved from that of **1**, but was almost equivalent to that of **2**, implying that glucose introduction at Ser⁷ had a negligible effect on recognition by degrading enzymes (Figure 2). Interestingly, the Ser(Glc)⁸ insertion (**6**) resulted in a large improvement: 70 % of **6** was still found intact after 24 h incubation. Therefore, existence of the Ser(Glc)⁸ played an important role in the enzymatic degradation due to the masking of the cleavage site by the large carbohydrate portion. Another possibility is that the observed improved metabolic stability of compound **6** can attribute to the existence of Leu⁷ and Trp⁹ next to the sterically hindered Ser(Glc): the sequence of Leu⁷-Ser(Glc)⁸-Trp⁹ in compound **6** has three bulky side-chains which should repel each other to form a rather fixed conformation at the C-terminus. This effect may be due to the insertion of large sugar portion in the appropriate position of the peptide and this conformational change should have some contribution to metabolic stability as well. Because of this improved metabolic stability together with the excellent and δ -selective bifunctional activities, **6** could be considered as the best derivative among **3-6**.

Conformational Analysis Based on ^1H NMR Studies in Membrane-mimicking Circumstances

As discussed previously,²⁰ the membrane-bound conformations of peptides has attracted interest recently, since the docking event of a ligand with its receptor, such as a GPCR, with its binding site in the transmembrane domain (such as opioid receptors and NK1 receptors), must take place near the membrane.^{45, 46} Hence, the transfer from solvent to cell membrane may be considered as an important step in a receptor-ligand binding event, and may be accompanied with a conformational change to a more biological relevant form, although it may differ from the binding conformation at the corresponding receptor.^{12, 15} Thus, the NMR structural analysis of **3-6** were performed to clarify the relationship between biological activity and conformation in membrane-mimicking environment in accord with the site-specific glycosylation in their peptide sequence.

Two-dimensional ^1H NMR studies including TOCSY, DQF-COSY and ROESY (for **3, 4** and **5**) or NOESY (for **6**) in pH 4.5 buffer (45 mM $\text{CD}_3\text{CO}_2\text{Na}/\text{HCl}$, 1 mM NaN_3 , 90% $\text{H}_2\text{O}/10\%$ D_2O) with a 40-fold excess of perdeuterated DPC micelles were performed on all four glycopeptide derivatives **3-6**. Nuclear Overhauser effects (NOEs) were measured using either 2D NOESY (optimal mixing time 450 ms) or 2D ROESY (150 ms), depending upon which method gave the larger number of cross-peaks. The NMR structure of **1** in the presence of DPC micelles was previously reported.²⁰ DPC is a widely used lipid-like surfactant to determine the solution NMR structures of membrane-bound proteins and peptides,^{20, 36, 37} and forms micelles above the critical micelle concentration.⁴⁷ All ^1H chemical shift assignments of **3-6** are listed in the Supporting Information.

Conformational Calculations

A large number of non-redundant NOE restraints (101, 110, 92 and 240 for **3, 4, 5** and **6**, respectively) were used for the conformational analysis. The interresidual NOE connectivities and the $^3J_{\text{HN-H}\alpha}$ coupling constants of all the peptide derivatives are illustrated in Figure 3.²⁰ Only $^3J_{\text{HN-H}\alpha}$ values of more than 8 Hz or less than 6 Hz were used for φ dihedral angle constraints,^{36, 37} and thus the numbers of applied dihedral angle constraints were 0, 2, 1 and 3 for **3, 4, 5** and **6**, respectively. Therefore, the total numbers of restraints were 101, 112, 93 and 243, corresponding to 10.1, 11.2, 9.3 and 22.1 restraints per residue (the *C*-terminal moiety and Glc were considered as residues). In the case of the observation of *cis/trans* isomers at the Pro⁶ residue, only the major isomer derived cross-peaks are considered in the structural calculation process, and all other amide bonds are fixed in the *trans* configuration (the detailed data are found in the Supporting Information).²⁰

The 20 lowest-energy structures from restrained molecular dynamics (rMD) calculations^{48, 49} were used for analysis of the glycopeptide derivatives **3-6** (Table 4). The superimposed images of the 20 structures are shown in Figure 4. The ensembles of structures for the glycopeptides derivatives **3-6** have small numbers of violations for total NOE restraints, maximum NOE distances and φ dihedral angles. The restraint energies derived from the Amber force field also were reasonably small (0.79, 0.68, 0.87 and 1.22 kcal mol⁻¹ for **3, 4, 5** and **6**, respectively). Since **2** showed similar biological activities as **1**, the sequence with Nle⁵ could be considered as equivalent to the one with Met⁵ in terms of the bioactive peptide conformation. Thus, the conformation of **1** will be used as the standard for comparison with the glycopeptide derivatives **3-6** throughout this discussion.

The calculated structures of **3**, which has a Ser(Glc) in the fifth position of the sequence in place of Met in **1**, showed larger rmsd values, especially for alignment on residues 1-4 (1.83 for backbone atoms and 2.41 for all heavy atoms; Table 4), than that of **1**. The rmsd values for the entire molecule also were increased from those of **1**, mostly because of the poorly-

defined opioid pharmacophore at the *N*-terminus. Its rmsd values with respect to residues 5-8 were small, however, and nearly the same to those of **1**. In the original definition, a structure in which the C_α of the *i*th residue and the C_α in the *i*+3rd residues are located less than 7 Å apart is considered a β-turn.⁵⁰ **3** had two β-turns common to **1** at residues 2-5 and 6-9 (Table 5). It should be noted that the distance between the C_α of Ser⁵ and the C_α of Trp⁸ also were within 7 Å, suggesting a different alignment of the same turn at the *C*-terminus. As a result, glycosylation at the residue 5 induced conformational changes to give a relatively less structured *N*-terminus (opioid pharmacophore) and an ordered *C*-terminus with rather structured β-turn structures (NK1 pharmacophore) in the pseudo-membrane circumstances. Interestingly, **3** had decreased affinities for the opioid pharmacophore, whereas the NK1 binding affinities of **3** were improved from those of **1** and **2** (Table 1).

When the site of glycosylation was shifted to residue 6 (**4**), the number of β-turn elements in the *N*-terminal half got smaller, whereas the distances between two C_α atoms for residues 4-7, 5-8 and 6-9 were less than 7 Å, indicating an apparent turn structure around these regions (Table 5). Since the two C_α atoms for residues 4-7 and 5-8 in **1** were larger than 7 Å, these secondary structural elements in **4** clearly were induced by the substitution of Pro⁶ by Ser(Glc). Generally, Pro is known as a turn-inducing amino acid, thus it is interesting that the Ser(Glc), but not the Pro residue, could yield such a β-turn-rich structure near the substituted site, possibly due to the large steric effect of the introduced sugar moiety. Although **4** had a large number of secondary structural elements in the ensemble of NMR structures, its structural definition was further decreased from those of **3** (the rmsd values for the whole molecule of **4** were 2.92 for the backbone atoms and 4.44 for all heavy atoms; Table 4). These results imply that Pro⁶ in **1** had an important contribution to its conformational stability. In fact, **4** had the least structured conformation among **3-6** and showed the lowest binding affinities at almost all the receptors tested (Table 1).

On the other hand, the introduction of Ser(Glc) at the seventh position (**5**) led to a more defined structure whose rmsd values (0.93 and 1.68 for backbone and all heavy atoms, respectively) were smaller than those of **1**, although the number of NOE restraints for **5** was the smallest among the tested peptides (Table 4). Interestingly, residues 1-4 had a rather extended and better-defined conformation than in **1**, but residues 5-8 did not, suggesting that the Ser(Glc)⁷ might act as an address region for the opioid agonist pharmacophore. The rmsd values of **5** were smaller than for **3** and **4**, with β-turn structural elements for residues 4-7 (Type I) and 6-9 (Type IV) (Table 5).

DPDPE (Tyr-*c*[*D*-Pen-Gly-Phe-*D*-Pen]OH) is a derivative of enkephalin and widely-used opioid agonist with high δ-selectivity over the μ receptor. In this compound, the structurally-fixed β-turn at residues 2-5 was found in its X-ray crystal structure,⁵¹ in the solution NMR structure⁵² and in the docking study at the δ opioid receptor.⁵³ Based on these observations, we hypothesized that this β-turn at residues 2-5 could be a key structure to enhance the δ-selectivity of enkephalin analogues. In fact, **5**, possessing an extended conformation in the opioid pharmacophore, has low δ-selectivity in terms of the binding affinities. Hydrogen bonds between glucose and Gly³ or Phe⁴ were observed in **5**, implying a direct interaction between Ser(Glc)⁷ and the *N*-terminal half that results in a fixed turn structure about residues 4-7 (Table 5 and 6). This interaction might play a part in the induction of the ordered *N*-terminal half of **5** that was observed. Collectively, the single substitution of Ser(Glc) at the 5, 6 or 7 residue of **2** led to diverse structural differences in their NMR structures in the membrane-mimicking environment depending on the site of glycosylation, but all of these glycopeptides **3-5** showed tandem-β-turn structures in the NK1 pharmacophores where the sugar was introduced, with more extended opioid pharmacophores.

Compared to the glycopeptide **5** with Ser(Glc)⁷, the derivative possessing Ser(Glc)⁸ (**6**) showed a further decrease in rmsd values, especially for backbone atoms (the rmsd value was only 0.13 for residues 1-4; Table 4), mostly owing to its structured *N*-terminus with a well-defined β -turn around residues 2-5. The better-defined structure of the *N*-terminus, as well as the smaller rmsd values, in the glycopeptide derivative **6** compared to **1-5** was also confirmed by the ϕ and ψ angular order parameters shown in Figure 5E and 5F.⁵⁴ It is worth mentioning that although the carbohydrate residue was inserted in the *C*-terminus, it led to a more structured *N*-terminus even though it is distant from the glycosylated position. Although the rmsd values of **6** decreased from those of **1**, the secondary structural elements of **6** were the same as those of **1**; both of these peptides had two β -turns, at residues 2-5 and at the *C*-terminus (Table 5). Interestingly, **6** had a well-defined β -turn at the residues 2-5 and showed good biological affinities for δ opioid receptors with the highest (39-fold) selectivity over the μ receptor among the tested peptides. Indeed, the insertion of a glycosylated moiety at the eighth residue gave rise to δ -selective opioid agonist and effective NK1 antagonist activities, presumably in relation to a structured conformation possessing two β -turns which were common to those in **1**. It should be noted that the glucose moiety in **5** and **6** should have a similar effect of masking their backbones from proteolytic enzymes, but only **6** showed improved metabolic stability compared to **2**. A possible explanation for this difference is that the ordered peptide conformation induced by the Ser(Glc)⁸ insertion could resist enzymatic cleavage of the peptide backbone. In fact, compound **6** has three bulky amino-acid residues in a row, Leu⁷-Ser(Glc)⁸-Trp⁹, for which a number of inter-residual NOE cross-peaks were found between Ser(Glc)⁸ and Leu⁷ (8 NOE cross-peaks) or Trp⁹ (21 NOE cross-peaks), suggesting a sequence with a rather fixed conformation at the *C*-terminus.

As observed in the Ramachandran plot, **5** possesses a Ser residue with positive ϕ and ψ angles in 14 out of the 20 best structures including the most stable one (Figure 5C). These positive ϕ angles of Ser⁷ in **5** with a bulky glucose could help drive its structure to be a β -turn near the glycosylated site, thus leading to the fixed *C*-terminal structures (Table 5). Gly³ was the other residue with positive ϕ angles; 14, 9, 10 and 20 ϕ angles for the best 20 structures were found positive at Gly³ for **3**, **4**, **5** and **6**, respectively (Figure 5A-D). It is interesting that **4** and **5**, with smaller numbers of β -turn elements in the *N*-terminal halves, had fewer positive ϕ angles at Gly³, whereas **3** and **6**, which had β -turns around residues 2-5 in which Gly³ was at the (*i* + 1) position, possessed a larger number of Gly³ with positive ϕ angles. Thus, these positive ϕ angles in the amino acid residues might be a good driving force to form secondary structural elements in the backbone, and could lead to a more ordered turn conformation, especially in **6**.

Paramagnetic Broadening Studies on ¹H NMR

In order to evaluate the mode of interaction of **6** with the model membrane, further NMR experiments using paramagnetic ions (Mn²⁺) were conducted in the presence of DPC micelles. The Mn²⁺ ions cause paramagnetic broadening and loss of resonance intensity of solvent-exposed protons observed as cross-peaks in the TOCSY spectra (Figure 6).²⁰ As a result of Mn²⁺ addition, all the resonances belonging to the backbone NH protons in **6** were eliminated except for that of Nle⁵, indicating that the backbone of **6** is located at the micelle surface, with only Nle⁵ buried inside the micelles. Most of the cross-peaks derived from protons in side-chains as well as in the *C*-terminus were preserved. It is reasonable that mostly lipophilic side-chains and the *C*-terminus interact with the lipophilic core of the micelles. These results for **6** were very similar to the observations for **1** in the same lipid-like environments.²⁰ Interestingly, cross-peaks related to the hydrophilic glucose were also preserved after Mn²⁺ addition, suggesting that the carbohydrate moiety is located inside the micelles. Thus, the introduction of a glycosylated residue at the eighth position did not

disturb the strong interaction of the peptide with membrane-mimicking micelles as observed in **1**, but provided a more structured conformation.²⁰ Since both the binding site of opioid and NK1 receptors were found in or near their transmembrane domains,^{42, 55} the ligand-membrane interaction should make an important contribution to the docking of the ligand at these receptors.

Conclusion

In order to obtain a novel type of analgesic compound with good metabolic stability, Ser(Glc) was introduced into the 5, 6, 7 and 8 position in the sequence of **2**. Among the synthesized derivatives, **6**, in which Ser(Glc) was inserted in between two bulky residues Leu and Trp in the sequence of **2**, showed improved metabolic stability compared to **2** in rat plasma. NMR structural analysis in the presence of DPC micelles indicated that this insertion of the sugar moiety into **6** led to a well-defined conformation with two β -turns at the residues 2-5 and the C-terminus, both of which were common to the previously observed conformation of **1**. In fact, the glycopeptides derivative **6** showed strong interactions with the model-membrane as previously observed for the non-glycosylated derivative **1**. The well-defined conformation and the existence of a large sugar portion in the sequence of **6** might play a part in its not being recognized by degrading enzymes. **6** also showed picomolar-level affinity for the hNK1 receptor and partial but effective agonist activity at the opioid receptors with improved δ -selectivity compared to that of **1**. Because of the improved metabolic stability, along with the bifunctional activities, **6** could be considered as a valuable research tool and possibly a promising candidate for a novel analgesic drug. The importance of these studies is that the site of glycosylation and the introduced steric repulsion with the neighboring residues are likely critical factors for the conformational and secondary structural elements of the peptide, both of which should have a significant contribution to biological recognition at a variety of proteins, including opioid receptors, NK1 receptors and several peptide-degrading proteases.

Experimental Section

Materials

All amino acid derivatives, coupling reagents and resins were purchased from EMD Biosciences (Madison, WI), Bachem (Torrance, CA), SynPep (Dublin, CA) and Chem Impex International (Wood Dale, IL). The 4-(4-Formyl-3-methoxyphenoxy)butyryl aminomethyl (FMPB-AM) resin was acquired from EMD Biosciences. Perdeuterated DPC was purchased from C/D/N Isotopes (Quebec, Canada). ACS grade organic solvents were purchased from VWR Scientific (West Chester, PA), and other reagents were obtained from Sigma-Aldrich (St. Louis, MO) and used as obtained. The polypropylene reaction vessels (syringes with frits) were purchased from Torviq (Niles, MI). Myo-[2-³H(N)]-inositol; [Tyrosyl-3,5-³H(N)] *D*-Ala²-Mephe⁴-glyol⁵-enkephalin (DAMGO); [Tyrosyl-2,6-³H(N)]-(2-*D*-Penicillamine, 5-*D*-Penicillamine)enkephalin (DPDPE); [³H]-substance P; and [³⁵S]-guanosine 5'-(γ -thio) triphosphate (GTP γ S) were purchased from Perkin Elmer (Wellesley, MA). Bovine serum albumin (BSA), protease inhibitors, Tris and other buffer reagents were obtained from Sigma (St. Louis, MO). Culture medium, Penicillin/ Streptomycin and fetal calf serum (FCS) were purchased from Invitrogen (Carlsbad, CA).

Peptide Synthesis

The glycopeptides (**3**, **4**, **5** and **6**) were synthesized by using reductive amination of 3,5-bistrifluoromethylbenzyl amine on FMPB-AM resin followed by the *N*^t-Fmoc solid-phase methodology. The FMPB-AM resin (675 mg, 0.50 mmol/g) was placed into a 50 mL polypropylene syringe with the frit on the bottom and swollen in DMF (20 mL) for 1 h. The

resin was washed with DMF (3×15 mL), and then the solution of 3',5'-bistrifluoromethylbenzyl amine (650 mg, 2.67 mmol) in the mixture of DMF (5 mL) and TMOF (5 mL) with 4 N HCl in 1,4-dioxane (0.6 mL, 2.40 mmol) was introduced. After shaking for overnight, the solution was eluted off and a solution of NaBH(OAc)₃ (508 mg, 2.40 mmol) in 5% AcOH in DMF (10 mL) was transferred into the reaction vehicle for 2 h. The resin was washed three times with DMF (15 mL) and three times with DCM (15 mL), and then with DMF (3×15 mL). The solution of 3',5'-bistrifluoromethylbenzyl amine (650 mg, 2.67 mmol) in DMF : TMOF = 1 : 1 (10 mL) with 4 N HCl in 1,4-dioxane (0.6 mL, 2.40 mmol) was prepared again, then added to the reaction vehicle for 2 h. The solution was filtered off, and the resin was treated with NaBH(OAc)₃ (508 mg, 2.40 mmol) in 5% AcOH in DMF (10 mL). After shaking for 1 h, the resin was washed with DMF (3×15 mL), DCM (3×15 mL) and DMF (3×15 mL). Fmoc-Trp(Boc)-OH (1.47 g, 2.79 mmol) and HCTU (1.15 g, 2.79 mmol) were dissolved in 15 mL of DMF, and then 2,6-lutidine (536 mg, 5.00 mmol) was added. The coupling mixture was transferred into the syringe with the resin and shaken overnight. The coupling was repeated for 2 h, and the unreacted amino groups were capped using acetic anhydride (2 mL) and pyridine (2 mL) in DCM (15 mL) for 30 min, then the resin was once again washed with DMF (3×15 mL), DCM (3×15 mL) and DMF (3×15 mL). The *N*^α-Fmoc protecting group was removed by 20% piperidine in DMF (20 mL, 1×2 min and 1×20 min). The deprotected resin was washed with DMF (3×15 mL), DCM (3×15 mL) and then with DMF (3×15 mL). The protected amino acid (3 equiv) and HCTU (2.9 equiv) were dissolved in 15 mL of DMF, then DIEA (6 equiv) was added. Fmoc-Ser(O-β-D-Glc(OAc)₄)-OH,⁴⁰ Fmoc-Leu-OH, Fmoc-Pro-OH, Fmoc-Nle-OH, Fmoc-Phe-OH, Fmoc-Gly-OH, Fmoc-D-Ala-OH and Boc-Tyr(tBu)-OH were used for respective coupling as protective amino acids. The coupling mixture was transferred into the reaction vehicle, and then shaken for 1.5 h. All the other amino acids were sequentially coupled using the procedure described above, using the TNBS test or chloranil test to check the extent of coupling. In case of a positive test result, the coupling was repeated until a negative test result was obtained. The resulting batch of resin-bound protected glycopeptide was carefully washed with DMF (3×15 mL), DCM (3×15 mL), DMF (3×15 mL), and DCM (3×15 mL), and dried under reduced pressure. After the glycopeptide was assembled on resin, the acetyl protecting groups of glucose moiety were removed with 80% H₂NNH₂-H₂O in CH₃OH (20 mL, 1×30 min and 1×1 h). The resin was washed three times with EtOAc (15 mL) and three times with DCM : CH₃OH = 1 : 1 (15 mL), then with DCM (3×15 mL). The cleavage of glycopeptide from the solid support was performed with the 3 mL of TFA/TIPS-OTf/thioanisole (9 : 2 : 1; v/v) for 45 min. The obtained crude glycopeptide was treated with chilled dry ether (45 mL) to give a dark oil. After centrifuge, the supernatant was decanted off, and then the crude glycopeptide was precipitated out with chilled dry ether (45 mL). The obtained yellow solid was dried under reduced pressure. The CH₃CN (5 mL) was added to the precipitated crude glycopeptide, and the solution was treated with 2 N NH₄F (2 mL) for 30 min. The solution was adjusted to pH 8.0 with triethylamine, stirred for 30 min at 0 °C, and then H₂O (20 mL) was added. CH₃CN was carefully titrated until the crude glycopeptide solution became clear which were subsequently passed through a C-18 reversed-phase silica gel column (Sep-Pak C18 cartridge, 5 g, Waters, Milford, MA) and the column was carefully washed by H₂O (40 mL). The glycopeptide absorbed on the column were eluted with CH₃CN (40 mL). The obtained solution was evaporated, and the residue was dissolved into H₂O : CH₃CN = 1 : 1 (5 mL) for the purification on Waters Delta Prep 4000 RP-HPLC system equipped with Waters XTerra C-18 column (19 × 250 mm, 10 μm, a linear gradient of 33-53%, 33-53%, 35-52% and 32-52% CH₃CN/0.1% TFA H₂O in 35 min for **3**, **4**, **5** or **6**, respectively at a flow rate of 15.0 mL/min) followed by lyophilizing. The final pure glycopeptides (>98 %) were characterized by analytical HPLC, ¹H-NMR, HRMS and TLC as previously described (available in the Supporting Information).¹⁹⁻²¹ ¹H-NMR studies showed *cis/trans*

isomerization about the X-Pro⁶. The ratios of two amide rotamers and their assignments also are available in the Supporting Information. The lyophilized product was a white amorphous solid.

In Vitro Stability of peptide derivatives in Rat Plasma⁵⁶

Stock solution of compounds (50 mg/mL in DMSO) were diluted 1000-fold into rat plasma (Lot 24927, Pel-Freez Biologicals, Rogers, AK) to give an incubation concentration of 50 µg/mL. All samples were incubated at 37 °C and 200 µL of aliquots were withdrawn at 1 min, 10 min, 30 min, 1 h, 2 h, 4 h, 6 h and 24 h (only for **6**). Then 300 µL of acetonitrile was added and the proteins were removed by centrifugation. The supernatant was analyzed for the amount of remaining parent compound by HPLC (Hewlett Packard 1090m with Vydac 218TP104 C-18 column; 4.6 × 250 mm, 10 µm, 300 Å). The samples were tested in three independent experiments (n = 3) and the mean values were used for the analysis with the SD.

NMR Spectroscopy in DPC amphipathic media and Conformational Structure Determination

All the conformational determinations were performed by the same methods as previously described,^{20, 36, 37} based on the NMR spectra using a Bruker DRX600 600 MHz spectrometer.

Briefly, the samples were prepared by dissolving the peptide (4 to 6 mM) in 0.5 mL of 45 mM sodium acetate-*d*₃ buffer (pH 4.5) containing 40 equivalents of dodecylphosphocholine-*d*₃₈ and 1 mM sodium azide (90% H₂O/10% D₂O) followed by sonication for 5 min. Two-dimensional double quantum filtered correlation (DQF-COSY), nuclear Overhauser enhancement spectroscopy⁵⁷ (NOESY, mixing time = 450 ms), Rotating frame Overhauser Effect Spectroscopy (ROESY, mixing time = 150 ms) and total correlation spectra⁵⁸ (TOCSY, MLEV-17 mixing time = 62.2 ms, spin-lock field = 8.33 kHz) were acquired using standard pulse sequences at 310 K. Coupling constants (³J_{NH-Hα}) were measured from 2D DQF-COSY spectra by analysis of the fingerprint region with a curve-fitting using 5-parameter Levenberg-Marquardt nonlinear least-squares protocol to a general antiphase doublet.

For conformational structure determination, the volumes of the assigned cross-peaks in the 2D NOESY spectrum were converted into upper distance bounds of 3.0, 3.8, 4.8, or 5.8 Å. For overlapping cross-peaks, the distance categories were increased by one or two levels, depending on the qualitative estimate of the extent of overlap. Pseudoatoms were created for nonstereospecifically assigned methylene protons with a correction of 1.0 Å applied to their upper bound distances.⁵⁹ In addition to the distance constraints, φ dihedral angle constraints derived from ³J_{NH-Hα} coupling constants were set to between -90 and 40° for ³J_{NH-Hα} < 6 Hz and to between -150 and -90° for ³J_{NH-Hα} > 8 Hz. Dihedral angle constraints of 180 ± 5° for peptide bonds (ω) were also used to maintain the planarity of these bonds. Simulated annealing molecular dynamics analysis was done for all the peptides to obtain an ensemble of NMR structures using NOE-derived distance constraints and dihedral angle (φ) constraints using the DGII⁶⁰ program within the software package Insight II 2000 (Accelrys Inc., San Diego, CA). The final 20 structures with the lowest energies were used for the analysis. All calculations were performed on a Silicon Graphics Octane computer.

Radioligand Labeled Binding Assay, [³⁵S]GTP-γ-S Binding Assay, GPI and MVD in Vitro Bioassay

The methods were carried out as previously described.¹⁹⁻²¹ Briefly, the evaluation of the binding affinities of the synthesized bifunctional peptide derivatives at the human δ-opioid

receptors (hDOR) and rat μ -opioid receptors (rMOR) were performed on the cell (HN9.10) membranes from cells that stably express these corresponding receptors using [3 H]-c[*D*-Pen², *D*-Pen⁵]-enkephalin ([3 H]DPDPE) and [3 H]-[*D*-Ala², NMePhe⁴, Gly⁵-ol]-enkephalin ([3 H]DAMGO) as the radioligands, respectively. [35 S]GTP γ S binding assays were used to estimate the functional activities for δ and μ opioid agonist efficacies on the same cell membrane. The isolated tissue-based functional assays also were used to evaluate opioid agonist activities in the GPI (δ) and MVD (μ). For the affinity at the human NK1 (hNK1) receptors, binding assays utilized membranes from transfected CHO cells that stably express hNK1 receptors, using [3 H]-substance P as the standard radioligand. The binding assay at the rat NK1 (rNK1) receptors also were performed using transfected CHO cells that stably express rNK1 receptors. To evaluate antagonistic activities against substance P stimulation, isolated tissue bioassays using GPI were performed in the presence of naloxone to block any opioid activities.

Supplementary Material

Refer to Web version on PubMed Central for supplementary material.

Acknowledgments

The work was supported by grants from the USDHS, National Institute on Drug Abuse, DA-13449 and DA-06284. We thank Dr. Guangxin Lin for kind assistance and advice with the NMR measurements, and Professor Robin Polt for discussions on glycosylated peptides, Ms. Magdalena Kaczmarek for culturing cells, the University of Arizona Mass Spectrometry Facility for the mass spectra measurements and Mr. Hajime Koganei for helpful scientific discussions. We express appreciation to Ms. Margie Colie and Ms. Brigid Blazek for assistance with the manuscript.

References

1. Witt KA, Davis TP. CNS drug delivery: opioid peptides and the blood-brain barrier. *Aaps J.* 2006; 8:E76–88. [PubMed: 16584136]
2. Albert R, Marbach P, Bauer W, Briner U, Fricker G, Bruns C, Pless J. SDZ CO 611: a highly potent glycosylated analog of somatostatin with improved oral activity. *Life Sci.* 1993; 53:517–525. [PubMed: 8341138]
3. Bilsky EJ, Eggleston RD, Mitchell SA, Palian MM, Davis P, Huber JD, Jones H, Yamamura HI, Janders J, Davis TP, Porreca F, Hruba VJ, Polt R. Enkephalin glycopeptide analogues produce analgesia with reduced dependence liability. *J Med Chem.* 2000; 43:2586–2590. [PubMed: 10891118]
4. Negri L, Lattanzi R, Tabacco F, Scolaro B, Rocchi R. Glycodermorphins: opioid peptides with potent and prolonged analgesic activity and enhanced blood-brain barrier penetration. *Br J Pharmacol.* 1998; 124:1516–1522. [PubMed: 9723966]
5. Polt R, Porreca F, Szabo LZ, Bilsky EJ, Davis P, Abbruscato TJ, Davis TP, Harvath R, Yamamura HI, Hruba VJ. Glycopeptide enkephalin analogues produce analgesia in mice: evidence for penetration of the blood-brain barrier. *Proc Natl Acad Sci U S A.* 1994; 91:7114–7118. [PubMed: 8041755]
6. Quartara L, Fabbri G, Ricci R, Patacchini R, Pestellini V, Maggi CA, Pavone V, Giachetti A, Arcamone F. Influence of lipophilicity on the biological activity of cyclic pseudopeptide NK-2 receptor antagonists. *J Med Chem.* 1994; 37:3630–3638. [PubMed: 7932590]
7. Hansch C, Dunn WJ III. Linear relationships between lipophilic character and biological activity of drugs. *J Pharm Sci.* 1972; 61:1–19. [PubMed: 4550859]
8. Susaki H, Suzuki K, Yamada H, Okuno S, Watanabe HK. Renal targeting of arginine-vasopressin by modification with carbohydrates at the tyrosine side chain. *Biol Pharm Bull.* 1999; 22:1094–1098. [PubMed: 10549862]
9. Suzuki K, Susaki H, Okuno S, Sugiyama Y. Renal drug targeting using a vector “alkylglycoside”. *J Pharmacol Exp Ther.* 1999; 288:57–64. [PubMed: 9862753]

10. Suzuki K, Susaki H, Okuno S, Yamada H, Watanabe HK, Sugiyama Y. Specific renal delivery of sugar-modified low-molecular-weight peptides. *J Pharmacol Exp Ther.* 1999; 288:888–897. [PubMed: 9918603]
11. Sargent DF, Bean JW, Schwyzer R. Conformation and orientation of regulatory peptides on lipid membranes. Key to the molecular mechanism of receptor selection. *Biophys Chem.* 1988; 31:183–193. [PubMed: 2852970]
12. Dhanasekaran M, Palian MM, Alves I, Yeomans L, Keyari CM, Davis P, Bilsky EJ, Egleton RD, Yamamura HI, Jacobsen NE, Tollin G, Hraby VJ, Porreca F, Polt R. Glycopeptides related to beta-endorphin adopt helical amphipathic conformations in the presence of lipid bilayers. *J Am Chem Soc.* 2005; 127:5435–5448. [PubMed: 15826181]
13. Egleton RD, Davis TP. Development of Neuropeptide Drugs that Cross the Blood-Brain Barrier. *NeuroRx.* 2005; 2:44–53. [PubMed: 15717056]
14. Egleton RD, Mitchell SA, Huber JD, Janders J, Stropova D, Polt R, Yamamura HI, Hraby VJ, Davis TP. Improved bioavailability to the brain of glycosylated Met-enkephalin analogs. *Brain Res.* 2000; 881:37–46. [PubMed: 11033091]
15. Palian MM, Boguslavsky VI, O'Brien DF, Polt R. Glycopeptide-membrane interactions: glycosylated enkephalin analogues adopt turn conformations by NMR and CD in amphipathic media. *J Am Chem Soc.* 2003; 125:5823–5831. [PubMed: 12733923]
16. Live DH, Williams LJ, Kuduk SD, Schwarz JB, Glunz PW, Chen XT, Sames D, Kumar RA, Danishefsky SJ. Probing cell-surface architecture through synthesis: an NMR-determined structural motif for tumor-associated mucins. *Proc Natl Acad Sci U S A.* 1999; 96:3489–3493. [PubMed: 10097062]
17. McManus AM, Otvos L Jr, Hoffmann R, Craik DJ. Conformational studies by NMR of the antimicrobial peptide, drosocin, and its non-glycosylated derivative: effects of glycosylation on solution conformation. *Biochemistry.* 1999; 38:705–714. [PubMed: 9888811]
18. Lis H, Sharon N. Protein glycosylation. Structural and functional aspects. *Eur J Biochem.* 1993; 218:1–27. [PubMed: 8243456]
19. Yamamoto T, Nair P, Davis P, Ma SW, Navratilova E, Moye M, Tumati S, Vanderah TW, Lai J, Porreca F, Yamamura HI, Hraby VJ. Design, Synthesis and Biological Evaluation of Novel Bifunctional C-terminal Modified Peptides for δ/μ Opioid Receptor Agonists and Neurokinin-1 Receptor Antagonists. *J Med Chem.* 2007; 50:2779–2786. [PubMed: 17516639]
20. Yamamoto T, Nair P, Jacobsen NE, Davis P, Ma SW, Navratilova E, Lai J, Yamamura HI, Vanderah TW, Porreca F, Hraby VJ. The Importance of Micelle-Bound States for the Bioactivities of Bifunctional Peptide Derivatives for δ/μ Opioid Receptor Agonists and Neurokinin 1 Receptor Antagonists. *J Med Chem.* 2008; 51:6334–6347. [PubMed: 18821747]
21. Yamamoto T, Nair P, Vagner J, Davis P, Ma SW, Navratilova E, Moye M, Tumati S, Vanderah TW, Lai J, Porreca F, Yamamura HI, Hraby VJ. A Structure Activity Relationship Study and Combinatorial Synthetic Approach of C-Terminal Modified Bifunctional Peptides That Are δ/μ Opioid Receptor Agonists and Neurokinin 1 Receptor Antagonists. *J Med Chem.* 2008; 51:1369–1376. [PubMed: 18266313]
22. King T, Gardell LR, Wang R, Vardanyan A, Ossipov MH, Malan TP Jr, Vanderah TW, Hunt SP, Hraby VJ, Lai J, Porreca F. Role of NK-1 neurotransmission in opioid-induced hyperalgesia. *Pain.* 2005; 116:276–288. [PubMed: 15964684]
23. Ma W, Zheng WH, Kar S, Quirion R. Morphine treatment induced calcitonin gene-related peptide and substance P increases in cultured dorsal root ganglion neurons. *Neuroscience.* 2000; 99:529–539. [PubMed: 11029544]
24. Powell KJ, Quirion R, Jhamandas K. Inhibition of neurokinin-1-substance P receptor and prostanoid activity prevents and reverses the development of morphine tolerance in vivo and the morphine-induced increase in CGRP expression in cultured dorsal root ganglion neurons. *Eur J Neurosci.* 2003; 18:1572–1583. [PubMed: 14511336]
25. Misterek K, Maszczyńska I, Dorociak A, Gumulka SW, Carr DB, Szyfelbein SK, Lipkowski AW. Spinal co-administration of peptide substance P antagonist increases antinociceptive effect of the opioid peptide biphalin. *Life Sci.* 1994; 54:939–944. [PubMed: 7511201]

26. Gu G, Kondo I, Hua XY, Yaksh TL. Resting and evoked spinal substance P release during chronic intrathecal morphine infusion: parallels with tolerance and dependence. *J Pharmacol Exp Ther.* 2005; 314:1362–1369. [PubMed: 15908510]
27. Dickenson AH. Plasticity: Implications for opioid and other pharmacological interventions in specific pain states. *Behav Brain Sci.* 1997; 20:392–403. [PubMed: 10097002]
28. Chang KJ, Rigdon GC, Howard JL, McNutt RW. A novel potent and selective nonpeptidic delta opioid receptor agonist BW373U86. *J Pharmacol Exp Ther.* 1993; 267:852–857. [PubMed: 8246159]
29. Sheldon RJ, Riviere PJ, Malarchik ME, Mosberg HI, Burks TF, Porreca F. Opioid regulation of mucosal ion transport in the mouse isolated jejunum. *J Pharmacol Exp Ther.* 1990; 253:144–151. [PubMed: 2329501]
30. Cowan A, Zhu XZ, Mosberg HI, Omnaas JR, Porreca F. Direct dependence studies in rats with agents selective for different types of opioid receptor. *J Pharmacol Exp Ther.* 1988; 246:950–955. [PubMed: 2901490]
31. Largent-Milnes, TM.; Yamamoto, T.; Davis, P.; Ma, SW.; Hruby, VJ.; Yamamura, HI.; Lai, J.; Porreca, F.; Vanderah, TW. Neuroscience. San Diego, CA: 2007. Dual acting opioid agonist/NK1 antagonist reverses neuropathic pain and does not produce tolerance. Poster 725. Visceral Pain: Transmitters and Receptors
32. Largent-Milnes, TM.; Yamamoto, T.; Nair, P.; Navratilova, E.; Davis, P.; Ma, SW.; Hruby, VJ.; Yamamura, HI.; Lai, J.; Porreca, F.; Vanderah, TW. Dual acting opioid agonist/NK1 antagonist peptide reverses neuropathic pain in an animal model without demonstrating common opioid unwanted side effects. International Association for the Study of Pain / 12th World Congress on Pain; Glasgow, Scotland. 2008.
33. Cirino PC, Tang Y, Takahashi K, Tirrell DA, Arnold FH. Global incorporation of norleucine in place of methionine in cytochrome P450 BM-3 heme domain increases peroxygenase activity. *Biotechnol Bioeng.* 2003; 83:729–734. [PubMed: 12889037]
34. Gilles AM, Marliere P, Rose T, Sarfati R, Longin R, Meier A, Fermandjian S, Monnot M, Cohen GN, Barzu O. Conservative replacement of methionine by norleucine in *Escherichia coli* adenylate kinase. *J Biol Chem.* 1988; 263:8204–8209. [PubMed: 2836418]
35. Sawyer TK, Sanfilippo PJ, Hruby VJ, Engel MH, Heward CB, Burnett JB, Hadley ME. 4-Norleucine, 7-D-phenylalanine-alpha-melanocyte-stimulating hormone: a highly potent alpha-melanotropin with ultralong biological activity. *Proc Natl Acad Sci U S A.* 1980; 77:5754–5758. [PubMed: 6777774]
36. Jacobsen NE, Abadi N, Sliwkowski MX, Reilly D, Skelton NJ, Fairbrother WJ. High-resolution solution structure of the EGF-like domain of heregulin-alpha. *Biochemistry.* 1996; 35:3402–3417. [PubMed: 8639490]
37. Ying J, Ahn JM, Jacobsen NE, Brown MF, Hruby VJ. NMR solution structure of the glucagon antagonist [desHis1, desPhe6, Glu9]glucagon amide in the presence of perdeuterated dodecylphosphocholine micelles. *Biochemistry.* 2003; 42:2825–2835. [PubMed: 12627948]
38. Matsumori N, Houdai T, Murata M. Conformation and position of membrane-bound amphotericin B deduced from NMR in SDS micelles. *J Org Chem.* 2007; 72:700–706. [PubMed: 17253784]
39. Dörner, B.; White, P. Peptides 1998, Proc 25th European Peptide Symposium. Bajusz, S.; H, F., editors. Akadémiai Kiadó; Budapest: 1999. p. 90
40. Seibel J, Hillringhaus L, Moraru R. Microwave-assisted glycosylation for the synthesis of glycopeptides. *Carbohydr Res.* 2005; 340:507–511. [PubMed: 15680608]
41. Millet R, Goossens L, Bertrand-Caumont K, Chavatte P, Houssin R, Henichart JP. Synthesis and biological evaluation of tripeptide derivatives of Cbz-Gly-Leu-Trp-OBzl(CF₃)₂ as NK1/NK2 ligands. *Lett Pep Sci.* 1999; 6:255–262.
42. Cascieri MA, Macleod AM, Underwood D, Shiao LL, Ber E, Sadowski S, Yu H, Merchant KJ, Swain CJ, Strader CD, Fong TM. Characterization of the interaction of N-acyl-L-tryptophan benzyl ester neurokinin antagonists with the human neurokinin-1 receptor. *J Biol Chem.* 1994; 269:6587–6591. [PubMed: 7509807]
43. Datar P, Srivastava S, Coutinho E, Govil G. Substance P: structure, function, and therapeutics. *Curr Top Med Chem.* 2004; 4:75–103. [PubMed: 14754378]

44. Millet R, Domarkas J, Rigo B, Goossens L, Goossens JF, Houssin R, Henichart JP. Novel potent substance P and neurokinin A receptor antagonists. Conception, synthesis and biological evaluation of indolizine derivatives. *Bioorg Med Chem.* 2002; 10:2905–2912. [PubMed: 12110311]
45. D'Alagni M, Delfini M, Di Nola A, Eisenberg M, Paci M, Roda LG, Veglia G. Conformational study of [Met5]enkephalin-Arg-Phe in the presence of phosphatidylserine vesicles. *Eur J Biochem.* 1996; 240:540–549. [PubMed: 8856052]
46. Deber CM, Behnam BA. Role of membrane lipids in peptide hormone function: binding of enkephalins to micelles. *Proc Natl Acad Sci U S A.* 1984; 81:61–65. [PubMed: 6320173]
47. Lazaridis T, Mallik B, Chen Y. Implicit solvent simulations of DPC micelle formation. *J Phys Chem B.* 2005; 109:15098–15106. [PubMed: 16852911]
48. Weiner SJ, Kollman PA, Case DA. An all atom force field for simulations of proteins and nucleic acids. *J Comput Chem.* 1986; 7:230–252.
49. Weiner SJ, Kollman PA, Case DA, Singh UC, Ghio C, Alagona GS, Profeta J, Weiner P. A New Force Field for Molecular Mechanical Simulation of Nucleic Acids and Proteins. *J Am Chem Soc.* 1984; 106:765–784.
50. Wagner G, Neuhaus D, Worgotter E, Vasak M, Kagi JH, Wuthrich K. Nuclear magnetic resonance identification of “half-turn” and 3(10)-helix secondary structure in rabbit liver metallothionein-2. *J Mol Biol.* 1986; 187:131–135. [PubMed: 3959079]
51. Flippen-Anderson JL, Hrubby VJ, Collins N, George C, Cudney B. X-ray Structure of [D-Pen2,D-Pen5]enkephalin, a Highly Potent, delta Opioid Receptor-Selective Compound: Comparisons with Proposed Solution Conformations. *J Am Chem Soc.* 1994; 116:7523–31.
52. Shenderovich MD, Kover KE, Nikiforovich GV, Jiao D, Hrubby VJ. Conformational analysis of beta-methyl-para-nitrophenylalanine stereoisomers of cyclo[D-Pen2, D-Pen5]enkephalin by NMR spectroscopy and conformational energy calculations. *Biopolymers.* 1996; 38:141–156. [PubMed: 8589249]
53. Feb. 2007 <http://www-personal.umich.edu/~him/modeling.htm>
54. Hyberts SG, Goldberg MS, Havel TF, Wagner G. The solution structure of eglin c based on measurements of many NOEs and coupling constants and its comparison with X-ray structures. *Protein Sci.* 1992; 1:736–751. [PubMed: 1304915]
55. Eguchi M. Recent advances in selective opioid receptor agonists and antagonists. *Med Res Rev.* 2004; 24:182–212. [PubMed: 14705168]
56. Hu X, Nguyen KT, Jiang VC, Lofland D, Moser HE, Pei D. Macrocyclic inhibitors for peptide deformylase: a structure-activity relationship study of the ring size. *J Med Chem.* 2004; 47:4941–4949. [PubMed: 15369398]
57. Kumar A, Ernst RR, Wüthrich K. A two-dimensional nuclear Overhauser enhancement (2D NOE) experiment for the elucidation of complete proton-proton cross-relaxation networks in biological macromolecules. *Biochem Biophys Res Commun.* 1980; 95:1–6. [PubMed: 7417242]
58. Davis DG, Bax A. Assignment of complex proton NMR spectra via two-dimensional homonuclear Hartmann-Hahn spectroscopy. *J Am Chem Soc.* 1985; 107:2820–2821.
59. Wüthrich K, B M, Braun W. Pseudo-structures for the 20 common amino acids for use in studies of protein conformations by measurements of intramolecular proton-proton distance constraints with nuclear magnetic resonance. *J Mol Biol.* 1983; 169:949–961. [PubMed: 6313936]
60. Havel TF. An evaluation of computational strategies for use in the determination of protein structure from distance constraints obtained by nuclear magnetic resonance. *Prog Biophys Mol Biol.* 1991; 56:43–78. [PubMed: 1947127]
61. Malicka J, G M, Czaplowski C, Kasprzykowska R, Liwo A, Lankiewicz L, Wiczak W. *Lett Pept Sci.* 1998; 5:445–447.
62. Toth G, Russell KC, Landis G, Kramer TH, Fang L, Knapp R, Davis P, Burks TF, Yamamura HI, Hrubby VJ. Ring substituted and other conformationally constrained tyrosine analogues of [D-Pen2,D-Pen5]enkephalin with delta opioid receptor selectivity. *J Med Chem.* 1992; 35:2384–2391. [PubMed: 1320122]

63. Mosberg HI, Hurst R, Hruby VJ, Gee K, Yamamura HI, Galligan JJ, Burks TF. Bis-penicillamine enkephalins possess highly improved specificity toward delta opioid receptors. *Proc Natl Acad Sci U S A*. 1983; 80:5871–5874. [PubMed: 6310598]
64. Wishart DS, Sykes BD, Richards FM. The Chemical Shift Index: A Fast and Simple Method for the Assignment of Protein Secondary Structure through NMR Spectroscopy. *Biochemistry*. 1992; 31:1647–1651. [PubMed: 1737021]
65. Andersen NH, Neidigh JW, Harris SW, Lee GM, Liu ZH, Tong H. Extracting Information from the Temperature Gradients of Polypeptide NH Chemical Shifts. 1. The Importance of Conformational Averaging. *J Am Chem Soc*. 1997; 119:8547–8561.

A List of Abbreviations

Abbreviations used for amino acids and designation of peptides follow the rules of the IUPAC-IUB Commission of Biochemical Nomenclature in *J. Biol. Chem.* **1972**, *247*, 977-83. The following additional abbreviations are used:

BBB	blood brain barrier
Boc	<i>tert</i> -butyloxycarbonyl
BSA	bovine serum albumin
Cl-HOBt	1-hydroxy-6-chlorobenzotriazole
CHO	Chinese hamster ovary
CNS	central nerve system
DAMGO	[<i>D</i> -Ala ² , NMePhe ⁴ , Gly ⁵ -ol]-enkephalin
DCM	dichloromethane
DIEA	diisopropylethylamine
DOR	δ opioid receptor
DPC	dodecylphosphocholine
DPDPE	c[<i>D</i> -Pen ² , <i>D</i> -Pen ⁵]-enkephalin
DQF-COSY	double quantum filtered correlation
FMPB-AM	4-(4-formyl-3-methoxyphenoxy)butyryl aminomethyl
Fmoc	fluorenylmethoxycarbonyl
GPI	guinea pig ileum
GTPγS	guanosine 5'-(γ-thio) triphosphate
HCTU	1H-Benzotriazolium-1-[bis(dimethylamino)methylene]-5-chloro-hexafluorophosphate-(1-),3-oxide
HRMS	high-resolution mass spectroscopy
LMMP	longitudinal muscle with myenteric plexus
MOR	μ opioid receptor
MVD	mouse vas deferens
NK1	neurokinin-1
NOE	nuclear Overhauser enhancement
NOESY	nuclear Overhauser enhancement spectroscopy

rMD	restrained molecular dynamics
rmsd	root mean square deviation
ROESY	rotating frame Overhauser effect spectroscopy
RP-HPLC	reverse phase high performance liquid chromatography
Ser(Glc)	<i>O</i> - β -glucosylated serine
SPPS	solid phase peptide synthesis
TFA	trifluoroacetic acid
TIPS-OTf	tirisopropylsilyl trifluoromethanesulfonate
TMOF	trimethyl orthoformate
TNBS	2,4,6-trinitrobenzene sulfonic acid
TOCSY	total correlation spectra
Trp-NH-3,5-Bzl(CF₃)₂	3',5'-(bistrifluoromethyl)-benzyl amide of tryptophan

NK1 pharmacophore

1: H-Tyr-*D*-Ala-Gly-Phe-Met-Pro-Leu-Trp-NH-3,5-Bzl(CF₃)₂

opioid pharmacophore

2: H-Tyr-*D*-Ala-Gly-Phe-Nle-Pro-Leu-Trp-NH-3,5-Bzl(CF₃)₂

3: H-Tyr-*D*-Ala-Gly-Phe-Ser(Glc)-Pro-Leu-Trp-NH-3,5-Bzl(CF₃)₂

4: H-Tyr-*D*-Ala-Gly-Phe-Nle-Ser(Glc)-Leu-Trp-NH-3,5-Bzl(CF₃)₂

5: H-Tyr-*D*-Ala-Gly-Phe-Nle-Pro-Ser(Glc)-Trp-NH-3,5-Bzl(CF₃)₂

6: H-Tyr-*D*-Ala-Gly-Phe-Nle-Pro-Leu-Ser(Glc)-Trp-NH-3,5-Bzl(CF₃)₂

Figure 1.
Sequences of opioid and NK1 receptor peptides.

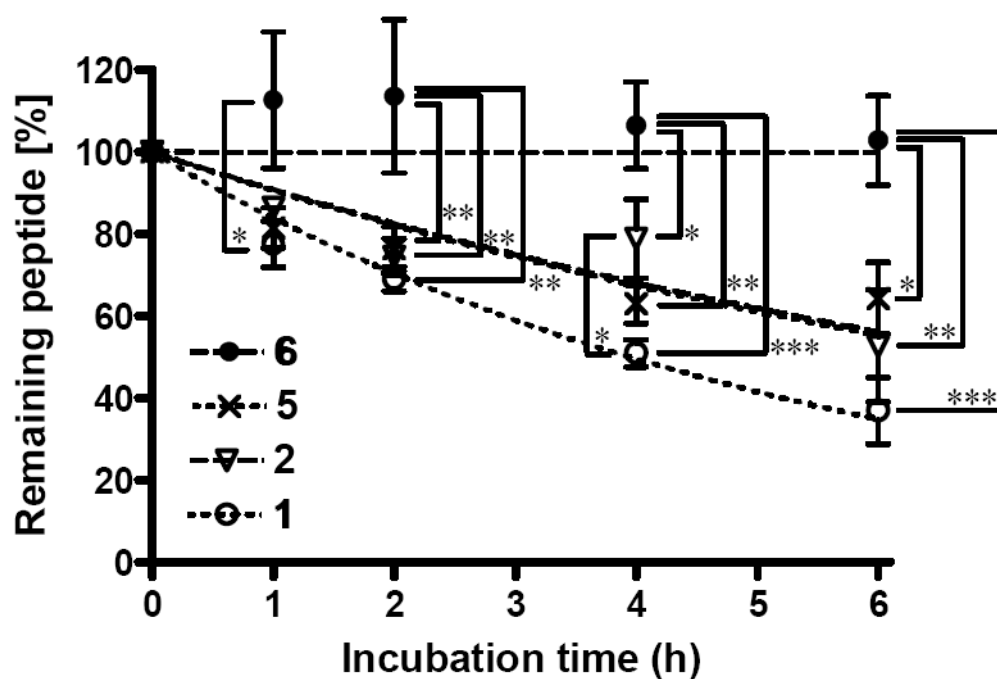


Figure 2. Comparison of the *in vitro* metabolic stability for **1** (open circle), **2** (open triangle), **5** (crossing) and **6** (filled circle) incubated in rat plasma at 37°C. Calculated half lives of peptide derivatives ($T_{1/2}$) were 4.8 h for **1** and > 6 h for **2**, **5** and **6**. 70 ± 9 % of **6** was found intact after 24 h incubation. The samples were tested in three independent experiments (n = 3) and the mean values were used for the analysis with the SD. Statistical significance was determined by Kruskal-Wallis test followed by Tukey's test. Asterisks denote significant differences (* $p < 0.05$; ** $p < 0.01$; *** $p < 0.001$).

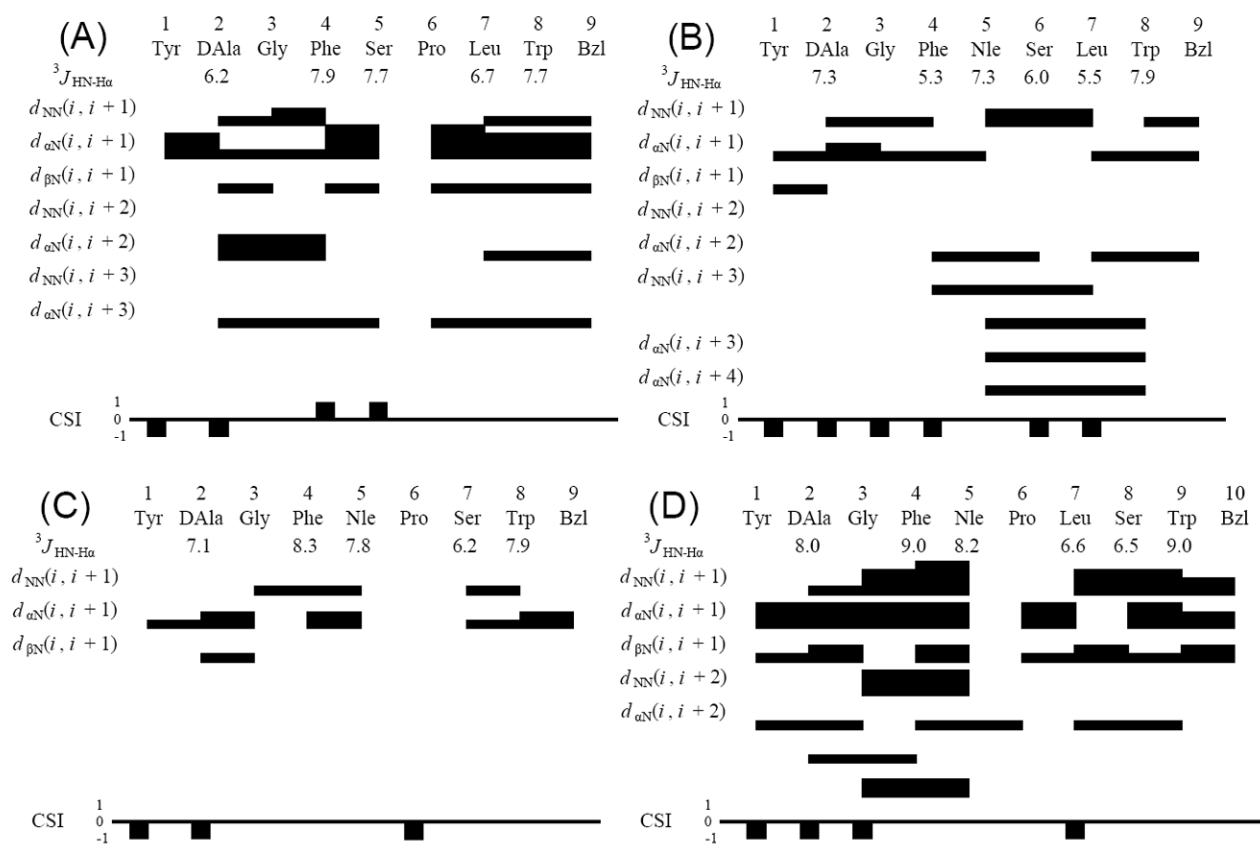


Figure 3. Diagram of $\text{H}^{\text{N}}\text{-H}^{\alpha}$ coupling constants, NOE connectivities, and H^{α} chemical shift index (CSI) for the (A) **3**, (B) **4** and (C) **5** and (D) **6**. The H^{α} CSI was calculated using the random-coil values reported by Andersen et al.^{64, 65}

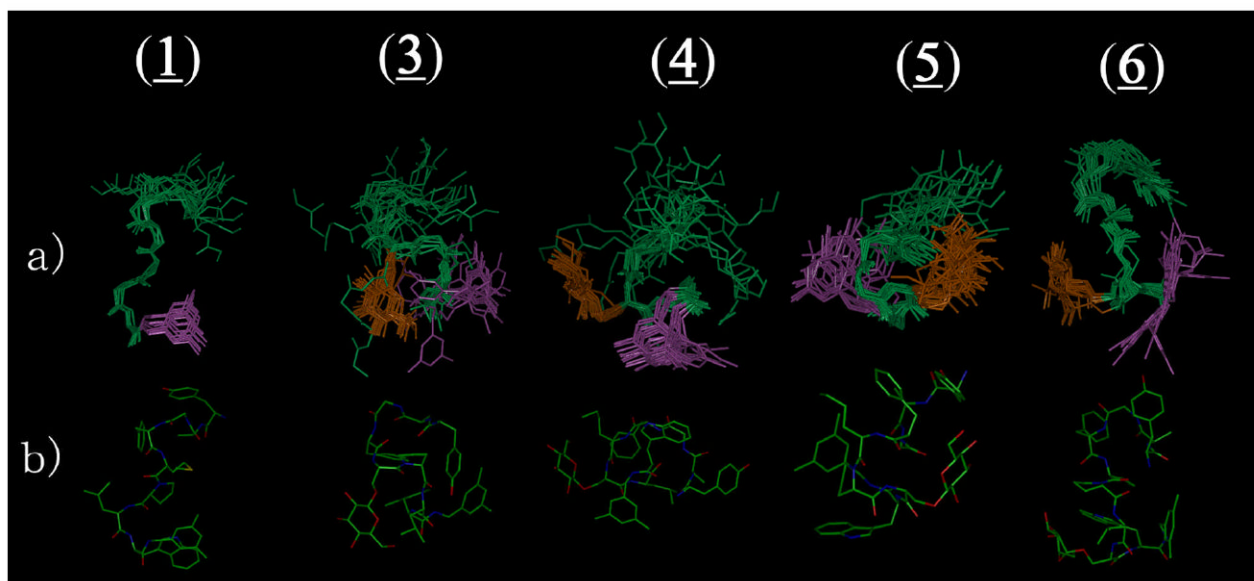


Figure 4. Ensembles of the best 20 calculated structures in 40-fold DPC micelle / pH 4.5 buffer for **1**,²⁰ **3**, **4**, **5** and **6**, respectively, with the lowest restraint energy, (a) aligned on backbone atoms of residues 5-8. The aligned structures are illustrated with the *C*-terminal benzyl moiety (purple) and glucose (orange). (b) The most stable conformers are shown with all heavy atoms (C, N and O).

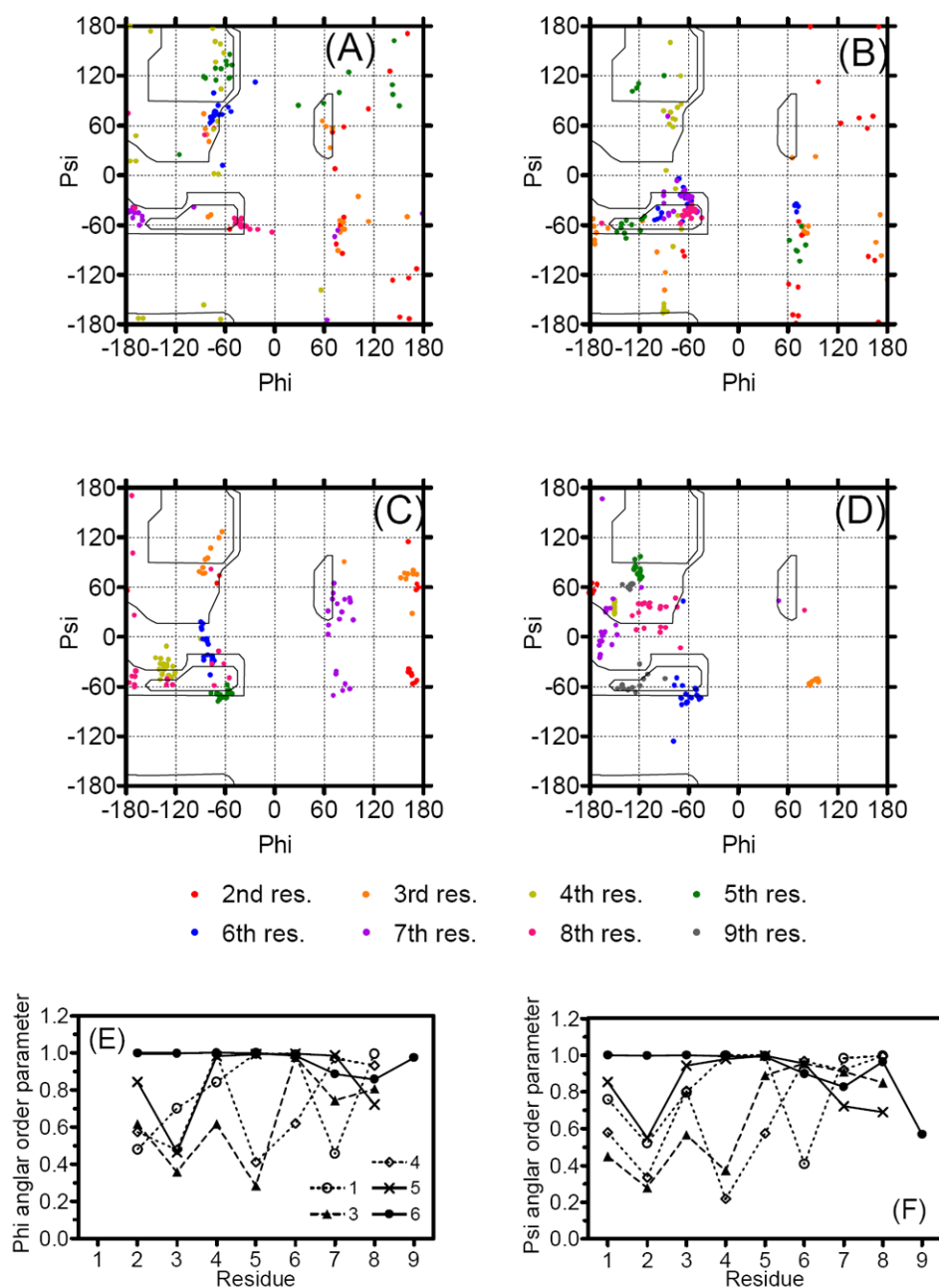


Figure 5.

The Glycosylated Ser (crosses) and Gly³ (open circle) were indicated in the Ramachandran ϕ, ψ plots for (A) **3**, (B) **4** and (C) **5** for residues 2-7 and (D) **6** for residues 2-8 of 20 final structures. Ser(OGlc) (crossing) and Gly³ (open diamond) were specified. The Nle⁵ with negative ϕ angle in **4** (circled) were illustrated in (B). Angular order parameters⁵⁴ for ϕ (E) and ψ (F) angles calculated from the 20 final structures for **1** (open circle),²⁰ **3** (filled triangle), **4** (open diamond), **5** (crossing) and **6** (filled circle), respectively. For calculating the ψ angles of Trp⁸, the nitrogen atoms of *C*-terminal benzyl amide were used instead of N ($i + 3$), respectively.

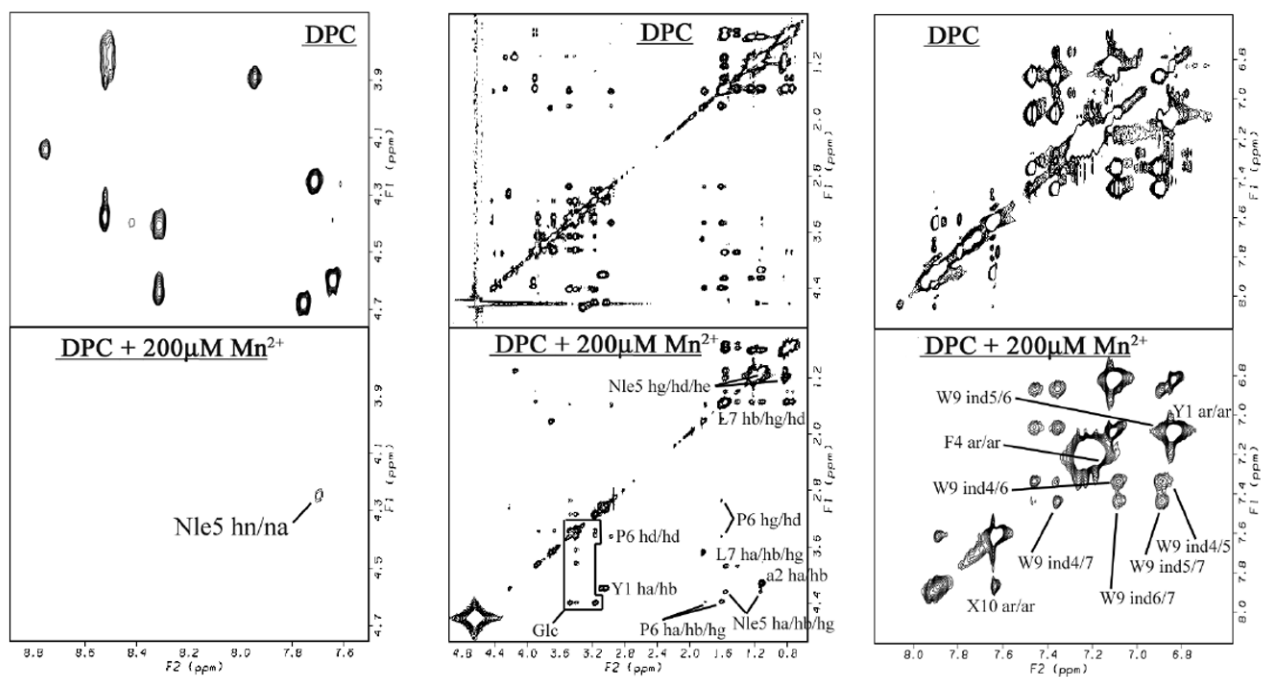


Figure 6.

The paramagnetic effects on TOCSY Spectra of **6. 6** with DPC micelles (top row) and with 200 μM Mn^{2+} (bottom). Preserved resonances (labeled) are in a phase not missed by the phase-specific radical probe (Mn^{2+}). Spectra were compared from the same noise level. X10 represents the cross-peaks derived from the corresponding aromatic protons of benzyl moiety.

Table 1
Binding affinities of bifunctional peptide derivatives at δ/μ opioid receptors and NK1 receptors

no	hDOR ^a , [³ H]DPPE ^b		rMOR ^a , [³ H]DAMGO ^c		K _i (μ)/K _i (δ)		hNK1 ^d , [³ H]Substance P ^e		rNK1 ^d , [³ H]Substance P ^f		K _i (hNK1)/K _i (rNK1)
	LogIC ₅₀ ^g	K _i (nM)	LogIC ₅₀ ^g	K _i (nM)	LogIC ₅₀ ^g	K _i (nM)	LogIC ₅₀ ^g	K _i (nM)	LogIC ₅₀ ^g	K _i (nM)	
1 ^h	-8.84 ± 0.07	0.66	-7.44 ± 0.05	16	-10.91 ± 0.10	0.0065	-7.61 ± 0.03	7.3	-7.61 ± 0.03	7.3	1100
2	-8.67 ± 0.05	1.0	-7.17 ± 0.07	32	-11.57 ± 0.59	0.0028	-7.68 ± 0.03	6.8	-7.68 ± 0.03	6.8	2400
3	-6.91 ± 0.09	59	-6.12 ± 0.15	260	-12.21 ± 0.61	0.0011	-8.35 ± 0.02	1.5	-8.35 ± 0.02	1.5	5600
4	-7.12 ± 0.09	36	-5.15 ± 0.20	3400	-8.38 ± 0.07	1.8	-7.14 ± 0.03	23	-7.14 ± 0.03	23	13
5	-8.10 ± 0.05	3.7	-7.77 ± 0.07	8.0	-9.75 ± 0.30	0.077	-7.30 ± 0.03	14	-7.30 ± 0.03	14	180
6	-8.83 ± 0.06	0.77	-7.22 ± 0.09	30	-9.93 ± 0.05	0.052	-7.02 ± 0.05	34	-7.02 ± 0.05	34	650
Biphalin ⁱ		2.6		1.4							
DPDPE/ ^j		1.6		610							
DPDPE/ ^k		10		3700							
L-732,138					-8.83 ± 0.02	0.73	-6.40 ± 0.03	130			180

^a Competition analyses were carried out using membrane preparations from transfected HN9.10 cells that constitutively expressed the δ and μ opioid receptors, respectively.

^b K_d = 0.45 ± 0.1 nM.

^c K_d = 0.50 ± 0.1 nM.

^d Competition analyses were carried out using membrane preparations from transfected CHO cells that constitutively expressed rat or human NK1 receptors.

^e K_d = 0.16 ± 0.03 nM.

^f K_d = 0.40 ± 0.17 nM.

^g The logIC₅₀ ± standard error are expressed as logarithmic values determined from the non linear regression analysis of data collected from at least two independent experiments performed in duplicate. The K_i values are calculated using the Cheng and Prusoff equation to correct for the concentration of the radioligand used in the assay.

^h Reference. 20

ⁱ Reference. 61

^j Reference. 20,62

^k Reference. 63

Table 2

Opioid agonist functional activities in [³⁵S]GTPγS binding assays

No	hDOR ^a			rMOR ^a		
	LogEC ₅₀ ^b	EC ₅₀ (nM) ^c	E _{max} (%) ^d	LogEC ₅₀ ^b	EC ₅₀ (nM) ^c	E _{max} (%) ^d
1 ^e	-8.07 ± 0.11	8.6	60 ± 2	-8.16 ± 0.17	7.0	51 ± 3
2	-8.30 ± 0.09	5.0	120 ± 3	-7.74 ± 0.14	18	66 ± 3
3	-7.29 ± 0.12	52	49 ± 2	-6.76 ± 0.31	180	24 ± 3
4	-7.56 ± 0.14	51	130 ± 3	-6.42 ± 0.19	380	81 ± 6
5	-8.10 ± 0.08	7.9	64 ± 2	-7.75 ± 0.23	18	38 ± 3
6	-7.56 ± 0.27	28	49 ± 3	-8.21 ± 0.24	6.2	50 ± 3
Biphalin	-8.95 ± 0.17	1.1	83			
DPDPE	-8.80 ± 0.25	1.6	69			
DAMGO				-7.44 ± 0.19	37	150

^aExpressed from HN9.10 cell.^bThe log EC₅₀ ± standard error are logarithmic values determined from the non-linear regression analysis of data collected from at least two independent experiments performed in duplicate.^cAnti-logarithmic value of the respective EC₅₀.^d $[(\text{Total bound} - \text{Basal})/(\text{Basal} - \text{Non-specific})] \times 100$ ^eReference.²⁰

Table 3
Functional assay results for bifunctional peptide derivative ligands at opioid and Substance P receptors

No	Opioid agonist			Substance P antagonist		
	MVD (δ)	Emax (%) ^b	IC ₅₀ (nM) ^a	GPI (μ)	Emax (%) ^b	Ke (nM) ^c
1 ^d	15 ± 2.0	100 ± 0	490 ± 29	92.5 ± 3.1	100 ± 0	10 ± 2.1
2	14 ± 1.6	100 ± 0	460 ± 160	100 ± 0	100 ± 0	10 ± 2.6
3	110 ± 21	100 ± 0	1900 ± 470	100 ± 0	100 ± 0	2.8 ± 0.73
4	18 ± 4.9	100 ± 0	250 ± 48	100 ± 0	100 ± 0	18 ± 6.0
5	13 ± 5.8	100 ± 0	520 ± 56	95.0 ± 2.9	100 ± 0	1.8 ± 0.30
6	17 ± 4.3	100 ± 0	670 ± 134	93.7 ± 4.1	100 ± 0	8.4 ± 1.0
Biphalin	2.7 ± 1.5		8.8 ± 0.3			
DPDPE ^e	4.1		7300			
DPDPE ^f	2.5		2720			
L-732,138						250 ± 87

^aConcentration at 50% inhibition of muscle contraction at electrically stimulated isolated tissues (n = 4).

^bThe δ and μ opioid agonist efficacies (Emax values) of tested compounds were calculated using DPDPE and PL-017 as standards (Emax = 100 %) for MVD and GPI assays, respectively.

^cInhibitory activity against the Substance P induced muscle contraction in the presence of 1 μ M naloxone. Ke: concentration of antagonist needed to inhibit Substance P to half its activity (n = 4).

^dReference.²⁰

^eReference.⁶²

^fReference.⁶³

Table 4

Atomic rmsd values (Å) for the final 19 conformers compared to the most stable conformer of bifunctional peptide derivatives.

	1 ^a	3	4	5	6
Backbone atoms (N, C ^α , C ^γ)					
Calculated on whole molecule	1.14 ± 0.43	2.04 ± 0.40	2.92 ± 0.67	0.93 ± 0.27	0.68 ± 0.30
Calculated only on 1-4 res.	1.05 ± 0.63	1.83 ± 0.43	1.38 ± 0.26	0.60 ± 0.33	0.13 ± 0.11
Calculated only on 5-8 res.	0.45 ± 0.38	0.48 ± 0.39	0.94 ± 0.22	0.56 ± 0.32	0.47 ± 0.23 ^c
all non-hydrogen atoms					
Calculated on whole molecule	2.09 ± 0.64	3.35 ± 0.86	4.44 ± 1.04	1.68 ± 0.44	2.01 ± 0.79
Calculated only on 1-4 res.	2.16 ± 0.98	2.41 ± 0.62	2.92 ± 0.54	0.78 ± 0.63	0.31 ± 0.40
Calculated only on 5-8 res. and C-terminus	1.02 ± 0.25	0.99 ± 0.60	1.56 ± 0.51	0.88 ± 0.35	0.57 ± 0.32 ^b

^aReference.²⁰

^bCalculated on 5-9 res. and C-terminus.

\$watermark-text

\$watermark-text

\$watermark-text

Table 5

Number of β -turn structural elements and the distance between alpha carbons of i th and $(i + 3)$ rd residues.^a

Residues	1 ^b		3		4		5		6	
	number of β -turns	distance (Å)	number of β -turns	distance (Å)	number of β -turns	distance (Å)	number of β -turns	distance (Å)	number of β -turns	distance (Å)
C ¹ α -C ⁴ α	3	7.86 ± 1.21	1	8.57 ± 0.62	3	8.08 ± 1.13	9	6.91 ± 0.41	0	
C ² α -C ⁵ α	20 ^c	4.95 ± 0.71	11 ^d	6.99 ± 1.08	6	7.00 ± 1.05	0		20	4.98 ± 0.33
C ³ α -C ⁶ α	0		8	7.39 ± 1.24	0 ^e		0		0	
C ⁴ α -C ⁷ α	0		0		17	5.37 ± 0.74	20 ^f	3.98 ± 0.23	0	
C ⁵ α -C ⁸ α	0 ^c		20 ^d	5.79 ± 0.39	17	5.46 ± 0.60	0		5 ^g	7.05 ± 0.16
C ⁶ α -Bzl	19	6.32 ± 0.43	11	6.96 ± 0.57	17 ^e	5.50 ± 0.36	18	6.56 ± 0.56	20 ^h	5.21 ± 1.02

^aOut of the best 20 calculated structures. The distance is the mean distance between two alpha carbons ± standard deviation (SD). The sequences with less than 7 Å distance between alpha carbons of i th and $(i + 3)$ rd residues without helical structure were considered as a β -turn.⁵⁰ Bzl stands for the benzyl moiety at the C-terminus.

^bReference.²⁰

Table 6

Hydrogen Bond Observed in the NMR structures of **3-6**.^a

Molecule	No. ^b	Donor	Acceptor	Distance (Å) ^c	Angle (deg) ^d
1^c	7	Gly ³ H ^N	Tyr ¹ O	2.05 ± 0.11	137.8 ± 8.1
	5	Trp ⁸ H ^N	Met ⁵ O	2.04 ± 0.02	132.3 ± 1.1
	9	Bzl ⁹ H ^N <i>f</i>	Pro ⁶ O	2.16 ± 0.11	158.5 ± 1.9
3	10	Phe ⁴ H ^N	DAla ² O	2.06 ± 0.09	144.1 ± 5.4
	7	Gly ³ H ^N	Tyr ¹ O	2.03 ± 0.08	142.8 ± 7.2
	16	Leu ⁷ H ^N	Ser ⁵ O	1.96 ± 0.05	132.1 ± 6.5
	13	Trp ⁸ H ^N	Ser ⁵ O	2.19 ± 0.12	151.4 ± 7.6
4	5	Glc H ^{O4}	Glc O ⁶	2.11 ± 0.02	127.3 ± 3.1
	8	Nle ⁵ H ^N	Gly ³ O	2.08 ± 0.16	138.3 ± 10.7
	8	Bzl ⁹ H ^{Ne}	Nle ⁵ O	1.97 ± 0.12	168.6 ± 9.5
	7	Bzl ⁹ H ^N	Ser ⁶ O	2.30 ± 0.12	132.8 ± 4.2
	11	Glc H ^{O2}	Bzl ⁹ F ^f	2.33 ± 0.05	150.6 ± 10.9
	6	Glc H ⁶	Glc O ⁴	2.19 ± 0.01	130.1 ± 0.3
	7	Glc H ^{O4}	Glc O ⁶	2.12 ± 0.03	129.8 ± 1.5
	6	Trp ⁸ H ^N	Pro ⁶ O	2.15 ± 0.13	144.8 ± 4.1
5	6	Glc H ^{O3}	Gly ³ O	2.25 ± 0.13	133.7 ± 6.3
	7	Glc H ⁶	Phe ⁴ O	1.96 ± 0.06	155.1 ± 9.3
	7	Glc H ^{O3}	Glc O ¹	2.28 ± 0.07	128.6 ± 4.5
6	13	Tyr ¹ H ^N	Nle ⁵ O	1.99 ± 0.04	137.4 ± 3.0
	20	Phe ⁴ H ^N	DAla ² O	2.22 ± 0.11	146.6 ± 2.3
	5	Glc H ^{O4}	Glc O ⁶	2.22 ± 0.06	129.3 ± 1.7

^aThe hydrogen bonds which were observed in more than five structures are listed.^bThe number of structures of the final 20 for which the listed hydrogen bond is observed.^cThe distance is the mean proton-acceptor atom distance (± SD) in the structures for which a hydrogen bond is observed.

\$watermark-text

\$watermark-text

\$watermark-text

^dThe angle is the mean angle (\pm SD) in the structures for which a hydrogen bond is observed.

^eReference. 20

^fAmide proton of C-terminal benzyl moiety. ^gFluorine atom of C-terminal benzyl moiety.